

Step Dynamics in 3D Crystal Shape Relaxation

K. Thürmer,¹ J. E. Reutt-Robey,² and Ellen D. Williams^{1,3}

¹*Department of Physics, University of Maryland, College Park, Maryland 20742-4111*

²*Department of Chemistry, University of Maryland, College Park, Maryland 20742-4111*

³*Institute for Physical Science and Technology, University of Maryland, College Park, Maryland 20742-4111*

M. Uwaha

Department of Physics, Nagoya University, Nagoya 464-8602, Japan

A. Emundts and H. P. Bonzel

Institut für Schichten und Grenzflächen, ISG3, Forschungszentrum Jülich, D-52425 Jülich, Germany

(Received 19 March 2001; published 10 October 2001)

Three-dimensional relaxation of small crystallites was imaged in real time using variable-temperature scanning tunneling microscopy. The micron-sized Pb crystallites, supported on Ru(0001), were equilibrated at 500–550 K, and the *volume-preserving* shape relaxation was induced by a rapid temperature decrease to 353–423 K. The (111) facet at the top of the crystallite grows by sequential peeling of single atomic layers, which shrink like circular islands. The rate of layer peeling slows dramatically as a new final state is reached.

DOI: 10.1103/PhysRevLett.87.186102

PACS numbers: 68.65.-k, 68.35.Fx, 68.35.Md, 68.37.Ef

With the relentless drive toward solid state structures of ever decreasing size scales, the issue of the stability of such structures, especially in response to external perturbations, becomes increasingly important. Real-time experimental observations of the complete decay of unstable structures, e.g., patterned Si substrates [1], nanofabricated Si mounds [2], and homoepitaxial islands [3–6] have clearly shown the discrete single-layer mode of decay. However, in complete contrast to these examples, we discuss for the first time the volume-preserving relaxation of a heteroepitaxial 3D crystallite from one well-defined state to another stable state, in response to a sudden change in chemical potential, here induced by an abrupt change in temperature. In relaxation, the ratio of forward and reverse flux is constantly decreasing, reaching a value of one in the final, equilibrium structure. This results in qualitatively different behavior than a decay process, where the forward flux is strongly dominating.

Figure 1 illustrates schematically the evolution of a faceted crystal from a stable high temperature state towards a low temperature state, causing the facet to grow. The thermodynamic driving force [7–12] for this process is well understood in terms of the increasing density of monatomic steps in the rounded regions of the crystallite near the facet [13] (a step is the boundary of a change in height by an atomic layer). In thermodynamic equilibrium, the ratio between facet radius ρ and the distance h of the facet from the center of the crystal is equal to the ratio of step free energy β to surface free energy γ of the facet [3,14]. With increasing temperature, steps lower their free energy by gaining configurational entropy due to kink formation [15] and by an excess vibrational free energy [5,16]. Since free energies for singular surfaces change much more slowly with temperature than step

free energies [17], a temperature increase corresponds to shrinking (and decrease to expansion) of the equilibrium facet diameter. Using linear kinetics, the rate of motion of a step will be proportional to the chemical potential change involved in removing an atom from the step's edge [18,19]. Using this approach, we define the chemical potential of the step bounding the top layer of a facet of radius ρ , as illustrated in Fig. 1, in terms of the curvature

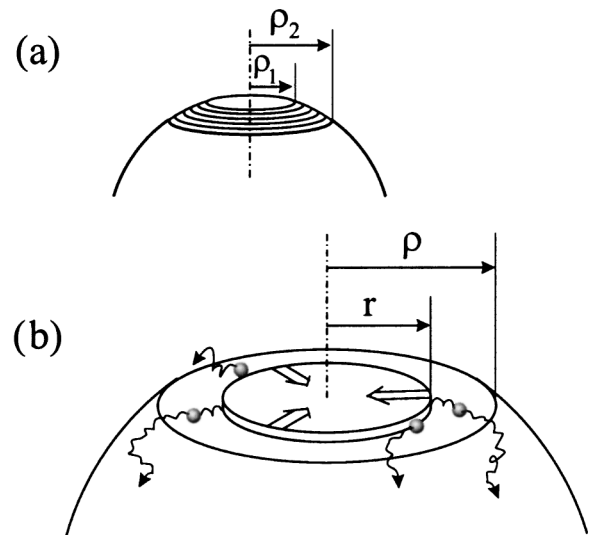


FIG. 1. Schematic crystal shape evolution upon temperature decrease: at elevated temperature the crystal is round with small (or no) facets, illustrated by a radius ρ_1 in (a). Lower layers on the crystallite have a larger radius, illustrated as ρ_2 in (a). With a temperature decrease, the total surface energy is reduced by an increase in facet size, leading to a reshaping process in which atomic layers peel off from the facet and their material is transferred to the rounded regions of the crystal surface.

of its edge and the repulsion from the neighboring step on the curved part of the crystallite [20,21],

$$\mu_s = \frac{\Omega \tilde{\beta}}{r} + \frac{2\Omega gh^3}{(\rho - r)^3}, \quad (1)$$

where Ω is the atomic area per atom on the facet, h is the step height, $\tilde{\beta}$ is the step stiffness, and g governs the step-interaction free energy. The top layer will shrink if the chemical potential of a step in the rounded vicinal region adjacent to the facet is lower than that of the step bounding the facet. A sudden change in temperature will create such an imbalance.

For these experiments we created 1–1.5 μm Pb crystals in UHV by room temperature deposition of a 20–30 nm Pb film onto a clean Ru(0001) substrate and subsequent dewetting at $T \approx 620$ K [22]. The liquid Pb droplets were solidified by applying a low cooling rate of 0.3 K/s to minimize crystal imperfections. Figure 2a shows a typical top facet of a crystal held for 2 days at $T = 382$ K and imaged at temperature with a variable temperature STM. The first atomically resolved images are direct proof of the (111) orientation of these defect-free top facets. Direct measurement of the shape of the rounded edge of such crystallites shows the 3/2 power law [23] expected for equilibrium shapes, showing that sufficient mass transport for local equilibration of the step configuration has occurred.

Next, we observed directly the evolution of the crystal shape following a drop of the sample temperature from about 550 K to temperatures where the surface mobility is expected to provide a convenient time scale. Figures 2b and 2c illustrate how the choice of $T = 353$ K permits monitoring shape relaxation in real time and with great detail: The series of STM images in Fig. 2b reveals that reshaping occurs via layer-by-layer peeling. The uppermost layer shrinks while maintaining a nearly circular shape. Only after it has vanished completely does the step loop of the now exposed next layer start to detach from the facet edge. The dots in the diagram of Fig. 2c represent the diameters of the top or second layers, taken from sequentially measured individual STM images. The decelerating repetition of (dot) chains in Fig. 2c shows the layer-by-layer process slowing down with time. The transient increase in the radius of the second layer just as the top layer disappears shows that a fraction of the material expelled from the top layer initially attaches to the second layer before it redistributes across the entire curved surface. Overall, the diameter of the (111) facet increases.

A simple physical picture captures much of the layer peeling kinetics of the crystallite. To describe the growth of a facet upon quenching, Uwaha [24] considered the flux of atoms between two concentric steps, neglecting at first the effect of step-step interactions and the redistribution of mass into the curved surface regions. Employing a quasistationary approximation for the distribution of

surface atoms for the diffusion-limited case, Uwaha [24] found the expression for the temporal evolution of the top layer radius r :

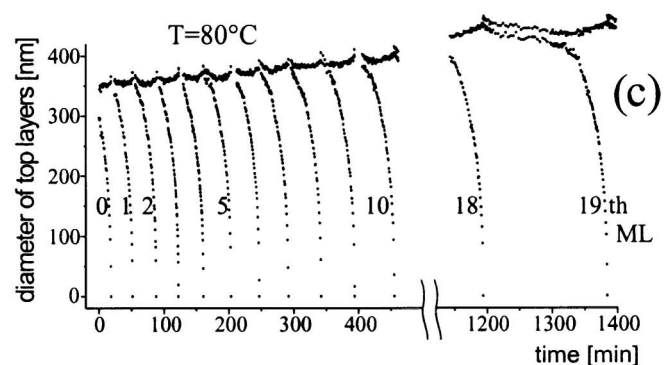
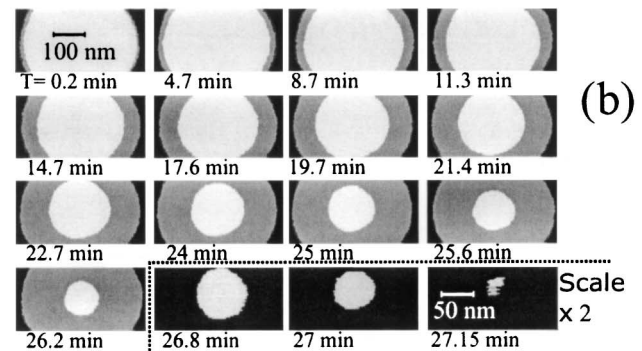
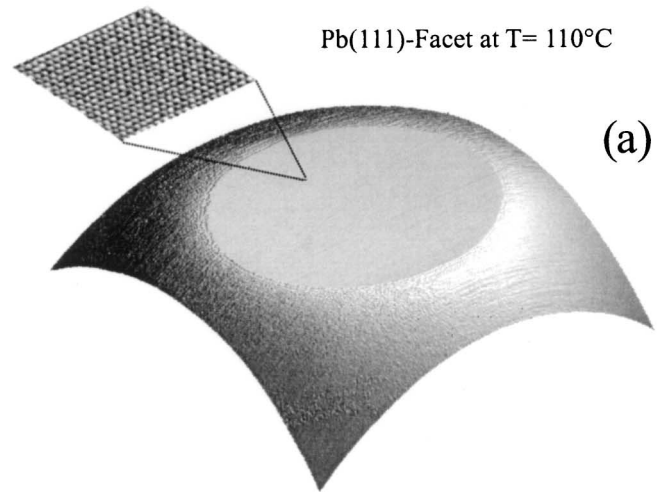


FIG. 2. (a) 750 nm \times 750 nm STM image of the top part of a supported Pb crystal acquired at $T = 383$ K. The crystal assumed this regular shape in two days of annealing at $T = 383$ K. The inset zooms into the top facet and shows the atomically resolved (111) surface. (b) Time sequence of STM images taken at 353 K. Scan areas: 400 nm \times 200 nm; last 3 images: 200 nm \times 100 nm. (c) Time evolution of the diameters of the two top atoms layers at 353 K. Time $t = 0$ is 8 h after the quench.

$$\frac{dr}{dt} = -\frac{D_s \lambda_\beta}{r \ln(\rho/r)} \left(\frac{1}{r} - \frac{1}{\rho} \right),$$

$$\text{with } \lambda_\beta = \Omega^2 c_0 \tilde{\beta} / kT, \quad (2)$$

where ρ is the radius of the step bounding the top facet (see Fig. 1b), D_s is the surface diffusion coefficient, and c_0 is the equilibrium adatom concentration for the (111) surface. Equation (2) was numerically integrated and fit to the later stage of the peeling curves of Fig. 3, where the distance between the edge of the shrinking layer and the next step is more than 30 nm, with the constraint of a common prefactor for all three curves. The late-stage fits, shown as solid lines at the right side of Fig. 3, illustrate the satisfactory agreement obtained with the prefactor $D_s \lambda_\beta$ equal to $1350 \text{ nm}^3/\text{s}$ at 353 K. The corresponding values for data (not shown) at $T = 368 \text{ K}$ and 423 K are 3700 and $110000 \text{ nm}^3/\text{s}$. In simple models, the quantities D_s , c_0 , and $\tilde{\beta}$ have an exponential form: $D_s = D_0 \exp(-E_D/kT)$, $c_0 \sim \exp(-E_B/kT)$, and $\tilde{\beta} \sim \exp(\varepsilon_{\text{kink}}/kT)$, with E_D the diffusion energy for an adatom on the (111) surface, E_B the formation energy for an adatom on the (111) terrace, and $\varepsilon_{\text{kink}}$ the energy of kink formation. The relative values of the prefactors at the three temperatures yield a value for $E_D + E_B - \varepsilon_{\text{kink}} = 0.86 \text{ eV}$. The magnitude of this number seems reasonable based on calculations of the surface energies [25], the kink energy of $\sim 60 \text{ meV}$ [22,23,25], and an estimate [26] of 100 meV for the activation energy of surface diffusion. Given the kink and activation energies, this result suggests that the value of the adatom formation energy is approximately 0.8 eV .

At the onset of peeling, the diffusion-limited model consistently overpredicts the rate of layer shrinking compared to the experimental observation (see offset of fits lines on left side of Fig. 3). This is primarily due to the neglect of step interactions and the redistribution of material over the

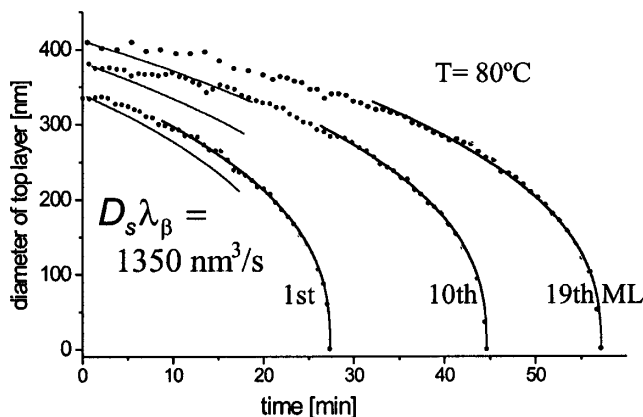


FIG. 3. Experimental evolution of the top layer diameter ($T = 353 \text{ K}$) and fits to the diffusion-limited model of Eq. (2). The same value of $D_s \lambda_\beta$ was used for all fits. The slower measured layer shrinking at the beginning compared to the calculation (straight lines) indicates the crossover to a more complex mechanism with correlated mass transfer among many layers adjacent to the facet.

curved vicinal region. The latter effect causes a transient surplus adatom density in the curved region near the facet edge, which generates a back flow [27] of atoms towards the top layer step and retards its collapse.

More globally, the physical properties governing the kinetics are revealed in the time envelope of the multilayer decay. The evolution of the height of the crystallite is fit most simply to an exponential relaxation, with a time constant of 780 min at 353 K , in contrast to the power-law form predicted and observed for the free decay of an unstable structure. In addition, the overall evolution of the shape of the Pb crystallite can be evaluated quantitatively by a plot of the time intervals Δt between disappearance of adjacent layers vs top-layer radius, such as shown by the solid symbols in Fig. 4a. The growth of the facet initially follows a power law $\Delta t \sim r^{2\beta}$, with $2\beta \sim 4.8$, and then slows exponentially, because of the decreasing gradient in chemical potential near the final stable state. In contrast, for the shape preserving decay of unstable or metastable structures, the evolution of the time interval Δt is expected to follow a power law with an exponent $2\beta = 3$ [2,21,24].

To demonstrate that a relaxation between high- and the low-temperature stable states can explain the observed temporal envelope, we use a formalism previously

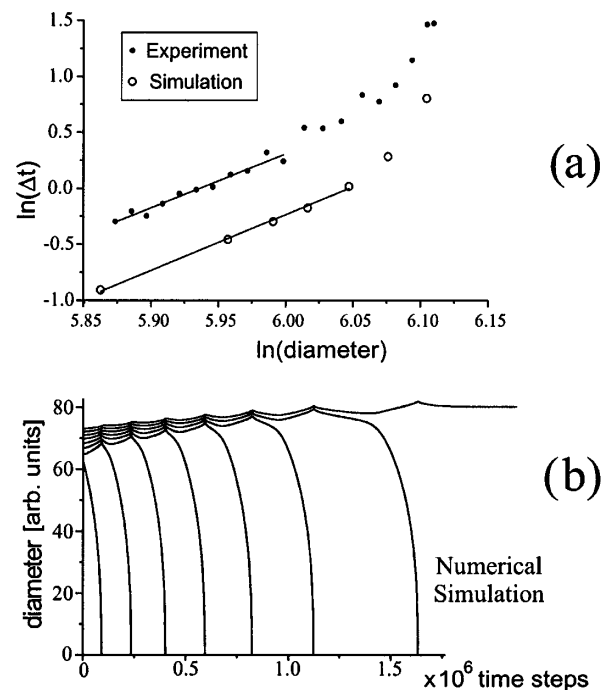


FIG. 4. (a) Evolution of the time difference Δt between adjacent layer disappearances, and the radius of the top facet. Solid symbols are experimental values for $T = 80^\circ\text{C}$, and open symbols are calculated values using the model described in the text. The solid lines show the power law fits with exponent 4.8 for the experimental data and 5.0 for the calculated points. (b) Calculated evolution of facet radius vs time for the relaxation of the structure to a final stable state using the model described in the text. Calculation parameters were $q = [1 + (K/D_s)(\Omega\tilde{\beta})/kT]^{-1} = 0.2$, where K is the step-attachment coefficient, and $G = (kT/\Omega\tilde{\beta})^3 \Omega g/kT = 0.01 \rightarrow 0.001$.

developed for the evolution of cylindrically symmetrical structures, including the effect of repulsive step-step interactions [20,21]. Parameters corresponding to diffusion-limited mass transfer were used in the calculations. The high temperature starting configuration is created numerically by allowing the relaxation of an arbitrary starting configuration (a cone), to a final state with strong step-step repulsions and a small step stiffness (e.g., a large value of the parameter G defined in the caption to Fig. 4). Then the value of G is reduced by a factor of 10, which creates a chemical potential imbalance equivalent to that caused by lowering the temperature. The calculated resulting relaxation of the simulated structure is shown in Fig. 4b. The essential features of the calculated relaxation, including the correlated motion in the first and second layers and the slowdown in the late stages, match the experimental observations (Fig. 2c) very well. A quantitative comparison of the rate of decay is shown in Fig. 4a, where the time intervals between successive calculated layer peelings are shown as open symbols. As with the experimental data, the calculation shows a regime of power-law behavior, followed by critical slowing down near the final state. The exponent observed for the calculated relaxation is $2\beta \sim 5.0$, close to the experimentally observed value of $2\beta \sim 4.8$. This is convincing corroboration that the quantitative value of the temporal exponent, as well as the critical slowing down near the final state, are the result of the physical mechanism being a relaxation between thermodynamic states, rather than a decay of a metastable or unstable state.

Another aspect of this problem, which we will address separately [28], is whether the final state is in global equilibrium or a metastable state. Specifically, the question is whether layer peeling stops because equilibrium has been reached, or whether an activation barrier prevents full equilibration [29,30]. However, interpretation of the kinetics of reshaping in terms of the step chemical potential requires only local equilibration, and thus is independent of the question of global equilibration.

The global aspects of reshaping outlined above define the framework in which mass transport from facets to the curved vicinal regions of 3D heteroepitaxial crystals takes place. For this relaxation process, a volume conserving material exchange among multiple steps occurs, with strong impact on the time scale of relaxation. The slowing down observed as the final stable state is approached is characteristic of a vanishing gradient in chemical potential near the final state. This causes interesting new scaling behavior, in which the temporal envelope of the relaxation is quantitatively different from that of decay.

This work has been supported by the NSF-MRSEC at University of Maryland under Grant No. DMR-00-80008. One of us (A.E.) is grateful to the DAAD for support. M.U. is supported by the "Research for the Future" program of the JSPS, and by the Japanese Ministry of Education.

- [1] S. Tanaka, N. C. Bartelt, C. C. Umbach, R. M. Tromp, and J. M. Blakely, *Phys. Rev. Lett.* **78**, 3342 (1997).
- [2] A. Ichimiya, K. Hayashi, E. D. Williams, T. L. Einstein, M. Uwaha, and K. Watanabe, *Phys. Rev. Lett.* **84**, 3662 (2000).
- [3] K. Morgenstern, G. Rosenfeld, E. Laegsgaard, F. Besenbacher, and G. Comsa, *Phys. Rev. Lett.* **80**, 556 (1998).
- [4] K. Morgenstern, G. Rosenfeld, G. Comsa, M. R. Sorensen, B. Hammer, E. Laegsgaard, and F. Besenbacher, *Phys. Rev. B* **63**, 045412 (2001).
- [5] M. Giesen and H. Ibach, *Surf. Sci.* **431**, 109 (1999).
- [6] P. Feibelman, *Surf. Sci.* **478**, L349 (2001).
- [7] M. Wortis, in *Chemistry and Physics of Solid Surfaces VII*, edited by R. Vanselow and R. F. Howe (Springer-Verlag, Berlin, 1988), p. 367, and references therein.
- [8] J. C. Heyraud and J. J. Métois, *J. Cryst. Growth* **50**, 571 (1980); *Surf. Sci.* **128**, 334 (1983); C. Rottman, M. Wortis, J. C. Heyraud, and J. J. Métois, *Phys. Rev. Lett.* **52**, 1009 (1984).
- [9] A. Pavlovskaya and E. Bauer, *Appl. Phys. A* **51**, 172 (1990); A. Pavlovskaya, D. Dobrev, and E. Bauer, *Surf. Sci.* **326**, 101 (1995).
- [10] H. P. Bonzel and A. Emundts, *Phys. Rev. Lett.* **84**, 5804 (2000), and references therein.
- [11] G. Wulff, *Z. Kristallogr. Mineral* **34**, 449 (1901).
- [12] C. Herring, *Phys. Rev.* **82**, 87 (1951).
- [13] A. F. Andreev, *Sov. Phys. JETP* **53**, 1063 (1981).
- [14] C. Jayaprakash and W. F. Saam, *Phys. Rev. B* **30**, 3916 (1984).
- [15] N. C. Bartelt, T. L. Einstein, and E. D. Williams, *Surf. Sci.* **240**, L591-L598 (1990).
- [16] M.-C. Desjonquères and D. Spanjaard, *Concepts in Surface Physics* (Springer-Verlag, Berlin, 1996), pp. 136ff.
- [17] E. D. Williams, *Surf. Sci.* **299/300**, 502 (1994).
- [18] P. Nozières, in *Solids Far from Equilibrium*, edited by C. Godreche (Cambridge University Press, Cambridge, United Kingdom, 1991), pp. 1–154.
- [19] H.-C. Jeong and E. D. Williams, *Surf. Sci. Rep.* **34**, 171 (1999).
- [20] N. Israeli and D. Kandel, *Phys. Rev. Lett.* **80**, 3303 (1998); *Phys. Rev. B* **60**, 5946 (1999).
- [21] M. Uwaha and K. Watanabe, *J. Phys. Soc. Jpn.* **60**, 497 (2000).
- [22] K. Arenhold, S. Surnev, H. P. Bonzel, and P. Wynblatt, *Surf. Sci.* **424**, 271 (1999).
- [23] A. Emundts, H. P. Bonzel, P. Wynblatt, K. Thürmer, J. Reutt-Robey, and E. D. Williams, *Surf. Sci.* **481**, 13 (2001).
- [24] M. Uwaha, *J. Phys. Soc. Jpn.* **57**, 1681 (1988).
- [25] P. Feibelman, *Phys. Rev. B* **62**, 17 020 (2000); H. S. Lim, *et al.*, *Surf. Sci.* **269–270**, 1109 (1992); R. J. Needs, M. J. Godfrey, and M. Mansfield, *Surf. Sci.* **242**, 215 (1991).
- [26] J. Frenken *et al.*, *Phys. Rev. B* **41**, 938 (1990).
- [27] J. Tersoff *et al.*, *Phys. Rev. Lett.* **70**, 1143 (1993).
- [28] K. Thürmer *et al.*, (to be published).
- [29] W. W. Mullins and G. S. Rohrer, *J. Am. Ceram. Soc.* **83**, 214 (2000); G. S. Rohrer, C. L. Rohrer, and W. W. Mullins (to be published).
- [30] N. Combe, P. Jensen, and A. Pimpinelli, *Phys. Rev. Lett.* **85**, 110 (2000).